Chinese Chemical Letters 33 (2022) 3017–3020

Contents lists available at ScienceDirect

Chinese Chemical Letters

journal homepage: www.elsevier.com/locate/cclet

Achieving a stable COF with the combination of "flat" and "twist" large-size rigid synthons for selective gas adsorption and separation

Jingyang Li[a], Ying He[b], Yongcun Zou[a], Yan Yan[a], Zhiguang Song[a,*], Xiaodong Shi[b,*]

[a] State key Laboratory of Supramolecular Structure and Materials, College of Chemistry, Jilin University, Changchun 130012, China
[b] University of South Florida, Tampa, FL 33620, United States

ARTICLE INFO

Article history:
Received 27 September 2021
Revised 28 November 2021
Accepted 5 December 2021
Available online 9 December 2021

Keywords:
N-2-Aryl triazole
ETTA
Covalent organic framework
Gas adsorption and separation

ABSTRACT

A new type of covalent organic framework (COF) was achieved using combination of structrally rigid and conformationally othorganal building blocks. The *N*-2-aryl-substituted triazole derivative (NAT-CHO) was prepared with co-planar conformation among the three aromatic rings as the "flat" building block. The 4,4′,4″,4‴-(ethene-1,1,2,2-tetrayl)tetraaniline) (ETTA) was applied as the "twist" building block. A 2D sheet of network was obtained through imine formation. The resulting NAT-COF gave excellent thermal and chemical stability, survived aqueous solutions from pH 5 to 13. With large-size building blocks, the porous framework NAT-COF gave efficient gas adsorption with excellent selectivity of C3 propane over C1 me-thane, suggesting its potential application for selective gas capture and separation.

As a new class of extended porous crystalline materials, covalent organic frameworks (COFs) have received tremendous attention in the past decades [1,2]. The covalent linkage along with high surface area, uniform pore size, thermal and chemical stabilities, and tunable structural properties make COF a promising material for applications in catalysis, drug delivery, gas storage, and separation [3–5]. The structure and function relationship of the resulting frameworks depends on versatile synthetic strategy to develop the linker between building blocks [6,7]. On the other hand, the geometry of building blocks determines both structural topology and functionality [8,9]. In general, structurally rigid building blocks are required to produce polymeric crystalline frameworks [10–12]. In addition, to reach controllable pore size, large building blocks are needed, which often requires long synthesis [13–15]. Therefore, new COF systems constructed from readily available building blocks with good porosity and adsorption selectivity are of great interest.

Among the literature reported polymerization strategies, aldehyde-amine condensation (formation of imine) is of the most popular approaches due to mild reaction condition (dehydration) and conformation control [16–19]. As shown in Scheme 1A, with aromatic aldehyde and aniline, the resulting Schiff base bearing extended conjugation of C=N with two arenes give good product stability. Moreover, although imine could give two different double isomers, the equilibrium nature of the reaction could lead to formation of more stable polymeric structures through building block conformation control [20–22]. Based on this strategy, various new COFs have been successfully prepared with interesting chemical and physical properties.

Clearly, the size and conformation of organic linker is crucial for the capability to form good COF materials [23–25]. To reach a desirable size of pore, rigid long linker is required. Linked aromatic hydrocarbon is one general strategy to achieve this goal. However, as shown in Scheme 1B, the arene could not form co-planar conformation due to the A-1,3 repulsion [26]. The resulted twisted conformation often caused repulsion between 2D network, making it less ideal linkage for COF synthesis. Full conjugated aromatic system, such as pyrene, has been used to overcome this problem by keeping the flat conformation with large distance between binding units [27–30]. However, the synthesis and derivatization of those compounds could be high cost and made it less practical for large scale COF production. Our group recently developed the *N*-2-aryltriazole (NAT) moiety as an alternative to reach co-planar conformation through readily available synthesis [31]. With this new conformationally rigid large linker, we proposed the combination of "flat" and "twisted" building blocks for construction of COF through simple Schiff-base formation process. Herein, we report the synthesis of a new COF from a flat building block NAT-CHO and a twisted building block ETTA amine. With these two readily available building blocks, NAT-COF could be easily prepared in large scale. This new organic framework showed excellent stability toward various solvents, acidic and basic aqueous solution (pH 5 to 13). The large pore size makes this new COF good material for

* Corresponding authors.
E-mail addresses: szg@jlu.edu.cn (Z. Song), xmshi@usf.edu (X. Shi).

https://doi.org/10.1016/j.cclet.2021.12.011
1001-8417/

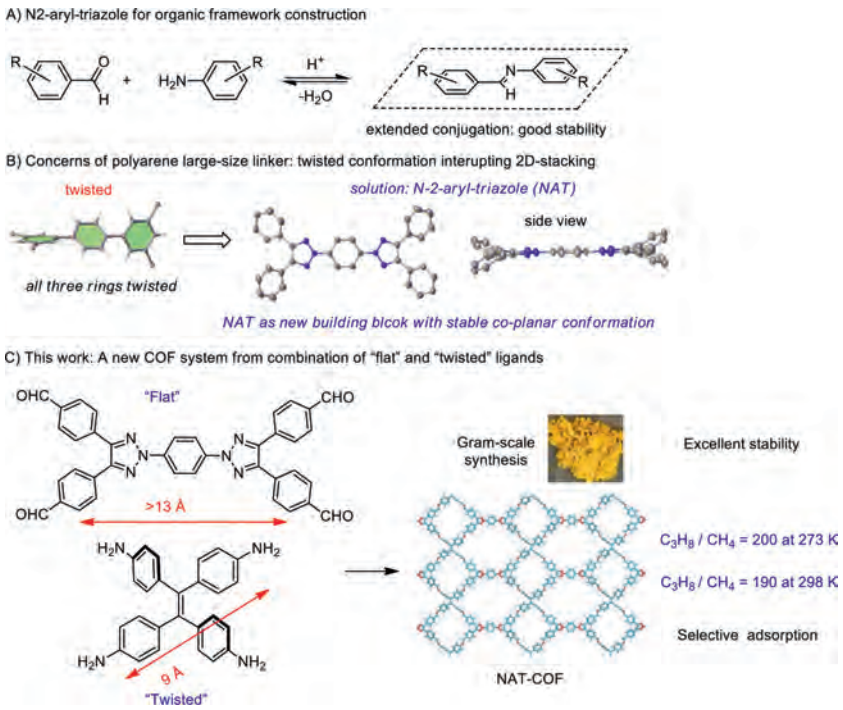

Scheme 1. NAT as the unique building block for material construction.

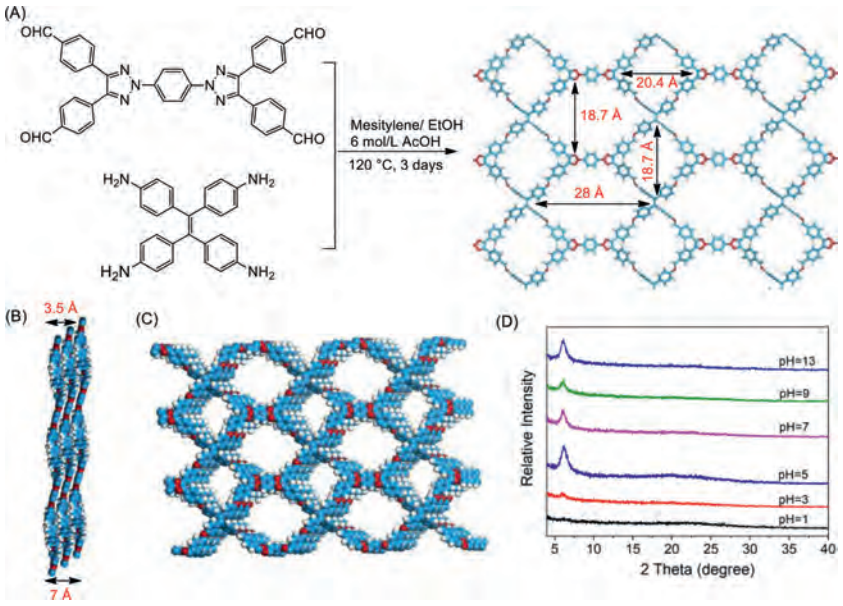

Fig. 1. (A) Synthesis of NAT-COF; (B) Side view of stacking of 2D NAT-COF; (C) Top view of stacking of 2D sheets; (D) Stability of NAT-COF in aqueous solution from pH 1 to pH 13 by PXRD.

gas adsorption, with 190:1 selectivity in adsorbing larger size C_3H_8 over CH_4 at 298 K, along with good adsorption selectivity toward CO_2 over N_2.

As shown in Fig. 1A, NAT-COF was synthesized with stoichiometric amount of NAT-CHO and ETTA in mixed solvents (mesitylene:EtOH:AcOH (6 mol/L) = 5:5:2, v/v/v) at 120 °C (Fig. 1A). After 3 days, yellow powder was obtained and washed by anhydrous THF, anhydrous trichloromethane and anhydrous methanol to obtain the pure NAT-COF powder in 90% yield. FT-IR was used to confirm imine formation (Fig. S3 in Supporting information). It can be found that characteristic C=N stretching at 1623 cm^{-1} formed while typical bands of C=O at 1703 cm^{-1} from NAT-CHO and N-H at 3357 cm^{-1} from ETTA almost disappeared after new material formation.

Having successfully obtained the NAT-COF, its crystal structure was simulated through Materials Studio (Fig. S2 in Supporting information). The simulated structure showed a 2D AA stacking structure which was linked by imine functional groups. In each layer, two pores were identified, suggesting this extended backbone could provide large porosity for promising gas sorption ability (Fig. 1A). Simulated NAT-COF from Materials Studio represents the stacking of layers with ordered pore channels of NAT-COF and the distance between neighboring layers was calculated to be around 3.5 Å (Figs. 1B and C).

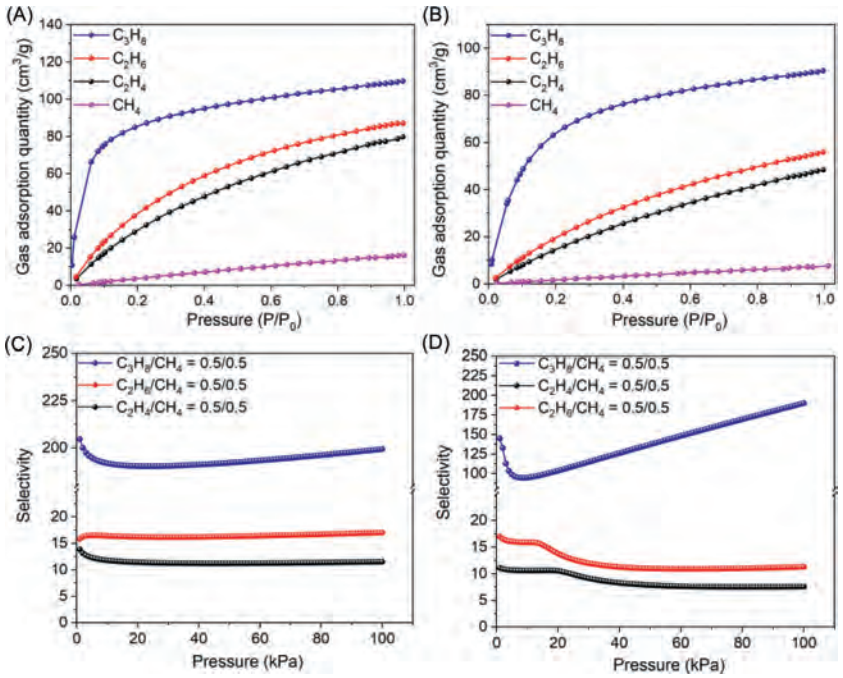

Fig. 2. Gas adsorption of C_3H_8, C_2H_6, C_2H_4 and CH_4 for NAT-COF at 273 K (A) and 298 K (B). Selectivity of C3 hydrocarbon over C1 for NAT-COF at 273 K (C) and 298 K (D).

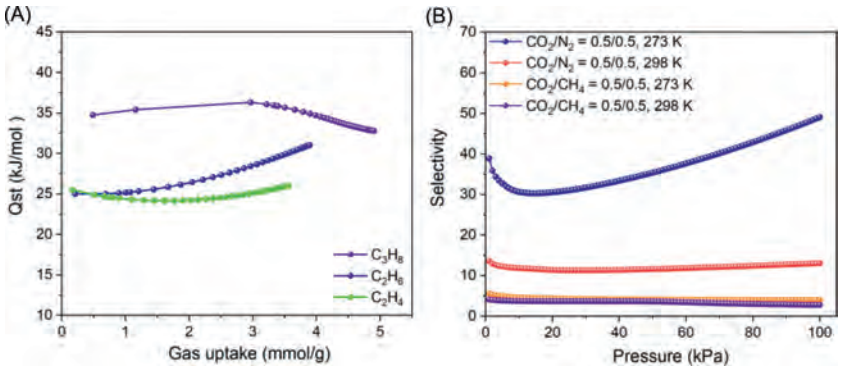

Fig. 3. (A) Q_{st} values of C_3H_8, C_2H_6 and C_2H_4; (B) Gas selectivity of CO_2 over CH_4 and CO_2 over N_2 at 273 K and 298 K.

To explore the property and functionality of this new network, we first evaluated its thermal and chemical stability. Thermogravimetric analyses (TGA) revealed good thermal stability of NAT-COF (Fig. S4 in Supporting information). Then the stability of COF in solution was investigated. NAT-COF was immersed in aqueous media with wide range of pH for 15 days at room temperature. The PXRD patterns showed that NAT-COF maintained the structural integrity from pH 5 to 13 (Fig. 1D). For organic solvents, NAT-COF maintained good stability in various organic solvents (acetone, MeOH, EtOH, DMF, DCM, MeCN and THF) after being immersed over 15 days at room temperature (Fig. S5 in Supporting information).

The porosity of NAT-COF was first examined by N_2 adsorption at 77 K using activated samples. The Brunauer-Emmett-Teller (BET) and Langmuir surface area were calculated to be 785.3 m^2/g and 945.6 m^2/g (Fig. S6 in Supporting information). Pore width distribution of NAT-COF suggests that NAT-COF contained both micropores and mesopores which facilitate gas adsorption (Fig. S7 in Supporting information).

Impurities from natural gas usually contain ethane and propane, which limited CH_4 utilization in natural-gas processing industry [32,33]. Considering good stability and moderate BET surface area, gas adsorption of NAT-COF for hydrocarbons including C_3H_8, C_2H_6, C_2H_4 and CH_4 at 273 K and 298 K were recorded with the trend of $C_3H_8 > C_2H_6 > C_2H_4 > CH_4$, highlighting the highest adsorption value of 109.8 cm^3/g (4.9 mmol/g) at 273 K and 90.4 cm^3/g (4.0 mmol/g) at 298 K for C_3H_8 among all tested gas, and detailed value for other gas are deposited in Figs. 2A and B).

The selectivity of gas molecules was calculated by Ideal solution adsorbed theory (IAST) with a good correlation factor ($R^2 > 0.999$). The selectivity curve of C3 hydrocarbon over CH_4 is shown in Figs. 2C and D. The results suggested a similar trend of $C_3H_8 > C_2H_6 > C_2H_4$ for the selectivity of C3 hydrocarbon over C1. The selectivity of C_3H_8/CH_4 is 200 at 273 K and 190 at 298 K. Both high sorption capability and selectivity towards C3 hydrocarbon over C1 could be attributed to size matching between C_3H_8 and large amount of micropores in the framework. Weak interactions between host and gas molecules (van der Walls forces) also have influenced on selectivity. Relatively more hydrophobic C3 hydrocarbon has stronger interaction with lipophilic ETTA. Isosteric heat of adsorption (Q_{st}) could also provide some insight for addressing this result. Q_{st} values C_3H_8, C_2H_6 and C_2H_4 were calculated and summarized in Fig. 3A. Among all tested gas, C_3H_8 gave the highest absolute Q_{st} value (34.7 kJ/mol) in all cases which could account for higher selectivity of C3 hydrocarbon over C1.

Carbon capture and sequestration (CCS) technology plays a crucial role in tackling environmental concerns related to growing at-

mospheric CO_2 emissions caused by fossil fuels [34–37]. Beside, CO_2 and CH_4 molecules have close kinetic diameters of 3.3 Å and 3.8 Å, which makes their separation *via* molecular sieving difficult. The nitrogen atoms in NAT-CHO could increase CO_2 adsorption capacity. Moderate selectivity between CO_2 and CH_4 (4 at 273 K and 2.8 at 298 K) was obtained (Fig. 3B), which can be contributed to higher Q_{st} value (Fig. S8 in Supporting information) of CO_2 (26.7 kJ/mol) compared with that of CH_4 (21.5 kJ/mol). Similarly, the selectivity of CO_2/N_2 is 49.1 at 273 K and 13.1 at 298 K, which is consistent with CO_2-philicity of NAT-COF owing to more dipole-dipole interactions.

In summary, combination of "flat" and "twisted" building blocks for the construction of COF was successfully achieved by tethering polar NAT-CHO and lipophilic ETTA through imine formation. Taking advantage of extended scaffold of co-planar NAT-CHO which was supported by "twisted" backbone of ETTA, NAT-COF exhibited excellent gas selectivity of hydrocarbons and CO_2. Notably, NAT-COF demonstrated efficient gas adsorption and selectivity in C3 propane over C1 methane, at the same time good with CO_2 over N_2, making it a promising candidate for both natural gas purification and CCS.

Declaration of competing interest

The authors declare that they have no known competing financial interests or personal relationships that could have appeared to influence the work reported in this paper.

Supplementary materials

Supplementary material associated with this article can be found, in the online version, at doi:10.1016/j.cclet.2021.12.011.

References

[1] T. Sun, J. Xie, W. Guo, D.S. Li, Q. Zhang, Adv. Energy Mater. 10 (2020) 1904199.
[2] X. Li, C. Yang, B. Sun, et al., J. Mater. Chem. A 8 (2020) 16045–16060.
[3] S.Y. Ding, W. Wang, Chem. Soc. Rev. 42 (2013) 548–568.
[4] X. Feng, X. Ding, D. Jiang, Chem. Soc. Rev. 41 (2012) 6010–6022.
[5] S. Lin, C.S. Diercks, Y.B. Zhang, et al., Science 349 (2015) 1208–1213.
[6] A.P. Cote, H.M. El-Kaderi, H. Furukawa, J.R. Hunt, O.M. Yaghi, J. Am. Chem. Soc. 129 (2007) 12914–12915.
[7] N. Huang, P. Wang, D. Jiang, Nat. Rev. Mater. 1 (2016) 16068.
[8] A. Nagai, Z. Guo, X. Feng, et al., Nat. Commun. 2 (2011) 536.
[9] P.J. Waller, F. Gandara, O.M. Yaghi, Acc. Chem. Res. 48 (2015) 3053–3063.
[10] D. Cao, J. Lan, W. Wang, B. Smit, Angew. Chem. Int. Ed. 48 (2009) 4730–4733.
[11] M.S. Lohse, T. Bein, Adv. Funct. Mater. 28 (2018) 1705553.
[12] H.S. Xu, S.Y. Ding, W.K. An, H. Wu, W. Wang, J. Am. Chem. Soc. 138 (2016) 11489–11492.
[13] H. Liao, H. Ding, B. Li, X. Ai, C. Wang, J. Mater. Chem. A 2 (2014) 8854–8858.
[14] S. Lu, Y. Hu, S. Wan, et al., J. Am. Chem. Soc. 139 (2017) 17082–17088.
[15] T.Y. Zhou, S.Q. Xu, Q. Wen, Z.F. Pang, X. Zhao, J. Am. Chem. Soc. 136 (2014) 15885–15888.
[16] S. Chandra, S. Kandambeth, B.P. Biswal, et al., J. Am. Chem. Soc. 135 (2013) 17853–17861.
[17] L. Li, F. Lu, R. Xue, et al., ACS Appl. Mater. Interfaces 11 (2019) 26355–26363.
[18] L. Pan, Z. Chen, W. Deng, G. Yan, X. Liu, Macromol. Res. 24 (2016) 366–370.
[19] X. Wang, R. Ma, L. Hao, et al., J. Chromatogr. A 1551 (2018) 1–9.
[20] Y. Peng, L. Li, C. Zhu, et al., J. Am. Chem. Soc. 142 (2020) 13162–13169.
[21] X. Chen, L. Xia, R. Pan, X. Liu, J. Colloid Interface Sci. 568 (2020) 76–80.
[22] X. Han, J. Zhang, J. Huang, et al., Nat. Commun. 9 (2018) 1294.
[23] C. Gao, G. Lin, Z. Lei, et al., J. Mater. Chem. B 5 (2017) 7496–7503.
[24] J. Wang, J. Li, M. Gao, X. Zhang, Nanoscale 9 (2017) 10750–10756.
[25] K. Yuan, C. Liu, L. Zong, et al., ACS Appl. Mater. Interfaces 9 (2017) 13201–13212.
[26] D. Bara, C. Wilson, M. Moertel, et al., J. Am. Chem. Soc. 141 (2019) 8346–8357.
[27] S. Dalapati, S. Jin, J. Gao, et al., J. Am. Chem. Soc. 135 (2013) 17310–17313.
[28] E. Jin, M. Asada, Q. Xu, et al., Science 357 (2017) 673–676.
[29] E. Jin, J. Li, K. Geng, et al., Nat. Commun. 9 (2018) 4143.
[30] G. Lin, H. Ding, D. Yuan, B. Wang, C. Wang, J. Am. Chem. Soc. 138 (2016) 3302–3305.
[31] J.Y. Li, Y. He, L. Wang, et al., Dalton Trans. 49 (2020) 5429–5433.
[32] H. Ma, H. Ren, S. Meng, et al., Chem. Commun. 49 (2013) 9773–9775.
[33] C.P. Xie, F. Huo, Y. Huang, et al., Part. Part. Syst. Charact. 34 (2017) 1600219.
[34] A.A. Olajire, J. CO_2 Util. 17 (2017) 137–161.
[35] N. Huang, X. Chen, R. Krishna, D. Jiang, Angew. Chem. Int. Ed. 54 (2015) 2986–2990.
[36] Z. Kang, Y. Peng, Y. Qian, et al., Chem. Mater. 28 (2016) 1277–1285.
[37] Y. Zeng, R. Zou, Y. Zhao, Adv. Mater. 28 (2016) 2855–2873.